Journal of Hydrology: Regional Studies 4 (2015) 131–153

Contents lists available at ScienceDirect

Journal of Hydrology: Regional Studies

journal homepage: www.elsevier.com/locate/ejrh

Brahmaputra river basin groundwater: Solute distribution, chemical evolution and arsenic occurrences in different geomorphic settings

Swati Verma [a], Abhijit Mukherjee [a,*], Runti Choudhury [b], Chandan Mahanta [b]

[a] Department of Geology and Geophysics, Indian Institute of Technology (IIT) – Kharagpur, West Bengal 721302, India
[b] Department of Civil Engineering, Indian Institute of Technology (IIT) – Guwahati, Assam 781039, India

ARTICLE INFO

Article history:
Received 1 November 2014
Received in revised form 11 February 2015
Accepted 8 March 2015
Available online 7 April 2015

Keywords:
Geomorphology
Arsenic
Groundwater
Himalaya
Brahmaputra
India

ABSTRACT

Study region: Brahmaputra River basin, India.
Study focus: The present study deciphers the groundwater solute chemistry and arsenic (As) enrichment in the shallow aquifers of the study region. Four different geomorphologic units, e.g. piedmont (PD), older alluvium of river Brahmaputra and its tributaries (OA), active alluvium of river Brahmaputra and its tributaries (YA) and river channel deposits (RCD) were identified. More than 62% of all groundwater samples collected have dissolved As >0.01 mg/L, whereas about 87% of groundwater samples in OA terrain are enriched with As, which draws a distinct difference from the adjoining Gangetic aquifers.
New hydrological insights for the region: Most groundwater solutes of RCD and YA terrains were derived from both silicate weathering and carbonate dissolution, while silicate weathering process dominates the solute contribution in OA groundwater. Groundwater samples from all terrains are postoxic with mean pe values between Fe(III) and As(V)–As(III) reductive transition. While, reductive dissolution of (Fe–Mn)OOH is the dominant mechanism of As mobilization in RCD and YA aquifers, As in OA and PD aquifers could be mobilized by combined effect of pH dependent sorption and competitive ion exchange. The present study focuses on the major ion chemistry as well as the chemistry of the redox sensitive solutes of the groundwater in different geomorphic settings and their links to arsenic mobilization in groundwater.

* Corresponding author. Tel.: +91 9007228876.
E-mail address: amukh2@gmail.com (A. Mukherjee).

http://dx.doi.org/10.1016/j.ejrh.2015.03.001

1. Introduction

Among the various organic and inorganic groundwater pollutants of recent times, geogenic groundwater arsenic (As) is observed as the most challenging contaminant in natural hydrological systems in a global scale (range from <1 μg/L to ~5000 μg/L in natural water) (Bhattacharya et al., 2002, 2006; Smedley and Kinniburgh, 2002; Mukherjee et al., 2008). The elevated concentrations of dissolved As in groundwater, higher than the World Health Organization (WHO) guideline value for drinking water of 10 μg/L, have been recognized in more than twenty geological provinces around the globe (Nriagu et al., 2007; Mukherjee et al., 2008). Most of the high As groundwater aquifers are located in parts of large sedimentary basins adjoining young mountain belts (Saunders et al., 2005; Naidu and Bhattacharya, 2009; Ravenscroft et al., 2009; Rahman et al., 2009; Mukherjee et al., 2014). Of these, the most extensive, As enriched aquifers are present in southeast Asia, which may be tectonically defined as foreland basins related to the Himalayan orogenic/Bhutan belt (Guillot and Charlet, 2007; Mukherjee et al., 2014). These include the Indus, Ganges and Brahmaputra river basins of Bangladesh, India, Nepal and Pakistan (Mukherjee et al., 2015). In most of these areas with As enriched groundwater, the aquifer sediments are of Quaternary age (Bhattacharya et al., 2001; Ahmed et al., 2004; Smedley, 2005; Nath et al., 2005; Charlet and Polya, 2006). The As enrichment in Ganges river basin (Bangladesh and Indian states of Bihar and West Bengal) have been very well studied for last three decades. In general, it was observed, that to a large extent, the distribution of the As-enriched aquifers are controlled by the geologic framework and geomorphic evolution of the river basins (Acharyya and Shah, 2007; Mukherjee et al., 2012, Diwakar et al., 2015). However, excluding very few publications available in the literature (e.g. Enmark and Nordborg, 2007; Bhattacharya et al., 2011; Chetia et al., 2011; Mahanta et al., 2015), the extent, distribution, origin, and mobilization process of As in the aquifers of river Brahmaputra basin, mostly located in the Indian state of Assam, has been largely undocumented, and unexplored.

Brahmaputra River (also known as Tsang Po in Tibet and China), the fourth largest fluvial system in the world, is the largest river that flow in the southeastern Tibet and northeastern parts of India, and is mostly responsible for landscape evolutions of associated region. Originated in the Trans-Himalayas, the river enters Indian state of the Assam through the deep Tsang Po gorge and flows as a wide and deep braided river system. The Brahmaputra river valley is mainly a Quaternary valley-fill with a few isolated pre-Cretaceous residual hills (Singh, 2005). In the Brahmaputra river basin, As enriched aquifers are located mostly in alluvial deposits by the Brahmaputra river channel and its tributaries (Chetia et al., 2011). In the present study, solute distribution and chemical evolution of groundwater and As enrichment of groundwater in part of the Brahmaputra basin, from near the eastern Himalayan foothills of Bhutan to the north bank of Brahmaputra river, is being studied in the perspective of the geomorphologic terrains.

2. Study area

The study area (Darrang and Udalguri districts), situated in the northwestern parts of Brahmaputra River basin of Assam (Fig. 1a), consists of braided alluvial flood plain deposits that are transported by the Brahmaputra river and its tributaries from the adjoining Himalayan provenance. The study area extends from north bank of Brahmaputra river to foothills or piedmont deposits of Eastern Himalayas near Bhutan–India Border. Tectonically, the study area is the eastern continuity of the Indo-Gangetic-Brahmaputra foreland basin of the Himalayas. In the study area, the northern tributaries of the river Brahmaputra drain through the southern slope of the Eastern Himalayas of Bhutan (Fig. 1a). The Brahmaputra river marks a boundary between the Pre-Cretaceous metamorphics and granites in the south and alluvial deposits in the north, up to the Himalayas. The geology of the Bhutan part of Eastern Himalayas comprises of Higher and Lesser Himalayas and the Siwaliks (Fig. 1a). All of the fluvial channels (Brahmaputra and its tributaries) in our study area flow through the strongly deformed Lesser Himalayan metasediments, composed of Precambrian limestone, dolostones, shale, quartzite and schists, along with gneisses and dolerite sills (Garzanti et al., 2004). The Siwalik is discontinuous in the eastern sections of the Himalayas, and includes a thick section of Neogene molasses. The Brahmaputra river basin sediments in the study area are mainly composed of alluvial deposits and it can be classified as older and younger alluvium. The older alluvium is exposed near or close to the

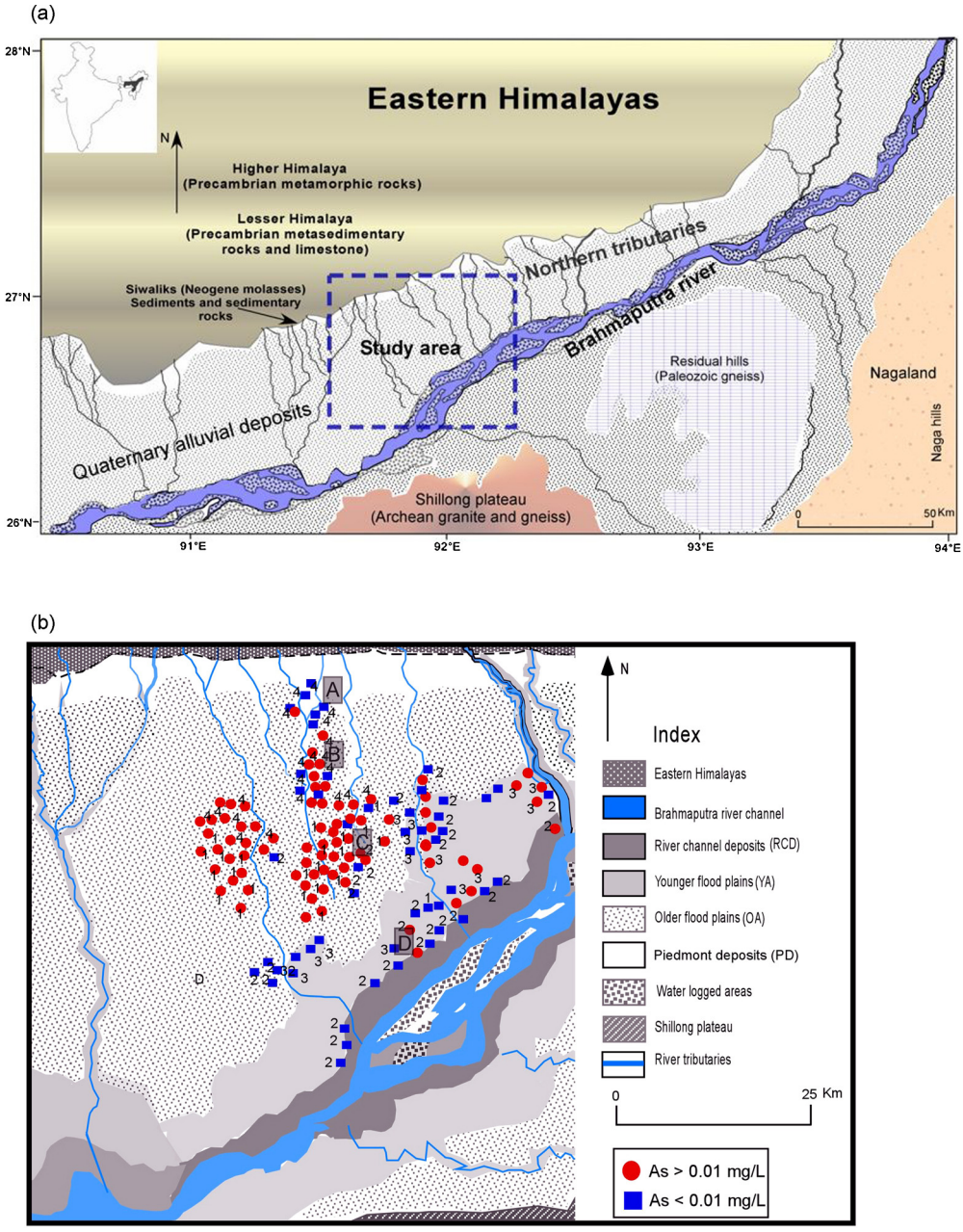

Fig. 1. Map of the study area showing (a) location of the study area, geomorphological and geological feature identified in study area by remote sensing and field observation; (b) showing sample locations classed by terrain type and arsenic concentrations and the numbers beside location are HCA clusters, A, B, C and D demonstrate location of lithologs.

Himalayan foothills in the northern side, and are comprised of sand, clay, pebble, gravel and boulder deposits. The younger alluvium is exposed along the present course of Brahmaputra river; marked by sand, silt and clay of relatively more recent age (Heroy et al., 2003). Rainfall in the study area takes

place mostly from southwest tropical monsoon, which is normally active from April to October. The annual average rainfall is ~1245 mm with maximum precipitation during June and July.

3. Methodology

Remote sensing and digital mapping have been used to investigate different geomorphic setting in study area from Landsat imagery, collected from NASA's GeoCover coverage GLS-2000. This involved an orthorectified, Landsat enhanced thematic mapper (ETM+), acquired on February 12, 2004, with a pixel resolution of 15 m. The imagery was collected on datum WGS 84 and projected on UTM 46. The delineated geomorphic features by the remote sensing were later finalized by extensive fieldwork and ground verification.

One hundred seven (107) groundwater samples from northwestern part of Brahmaputra river basin (Darrang and Udalguri district, Assam) and northern bank aquifers of the river were collected from hand-pumped and public water supply wells following procedures of Mukherjee and Fryar (2008) between February and March 2013. The groundwater samples have been taken from various depths ranging from 7 to 60 m below ground level (bgl) but normally <50 m bgl. All of the groundwater samples represented the shallow aquifers system in the study area. The collection of groundwater samples and field measurements were done by standard hydrogeochemical procedures (Wood, 1981). Groundwater samples were abstracted from the wells after purging for several well volumes in order to obtain representative samples. Under minimal atmospheric contact, field parameters like E_H, temperature, pH, dissolved O_2 (DO) and specific conductance (EC) were measured by using a multiparameter probe (Hanna 9282) after stabilization of field parameters. After collection, all groundwater samples were filtered by 0.45-μm filters. Samples for cations (major and trace) were collected and preserved by acidification with 6 N HNO_3 in the field to pH ~2. Samples for HCO_3^- analysis were collected without adding any preservative and $CHCl_3$ used as preservative for other anion in water samples (Böttcher et al., 1990). Total alkalinity (as HCO_3^-) was calculated by titration by using the US Geological Survey alkalinity calculator (http://or.water.usgs.gov/alk). Samples for ^{18}O and ^{2}H were collected in 8-mL HDPE bottles without adding any preservative and without headspace. Major anions were measured by ion chromatography in the hydrogeology laboratory of IIT Kharagpur. The major cations and trace metal have been measured by inductively coupled plasma with optical emission spectrophotometer (ICP-OES, Thermo Fisher ICAP 6000). Precision for most of the analyses was better than 3%. Stable isotopes were analyzed by using a continuous-flow isotope-ratio mass spectrometer (CF-IRMS) for $\delta^{18}O$ and Dual inlet isotope-ratio mass spectrometer (DI-IRMS) for $\delta^{2}H$. Precision (1ρ) was ±0.1‰ (VSMOW) for $\delta^{18}O$, ±1.0‰ (VSMOW) for $\delta^{2}H$.

Multivariate statistical method (hierarchical cluster analyses [HCA]) has been used to investigate relationships among solutes of the samples by using the statistical software package SPSS version 16. The analyses were done on the original data set without any weighting or standardization. The HCA was performed on the concentrations of As, Ca, Fe, K, Mg, Mn, Na, Zn, Cl, NO_3, SO_4, HCO_3, EC, pH, E_H for each location. The HCA dendrogram was constructed by Ward's method (Ward, 1963). The principal component axes were rotated using a varimax algorithm for simplified visualization.

Saturation indices ($SI = \log[IAP\, K_T^{-1}]$), where IAP is the ion activity product and K_T is the equilibrium solubility constant of a mineral phase at ambient temperature were calculated for all groundwater samples of four different terrains the using PHREEQC version 3.0. The geochemical program, PHREEQC, based on the database WATEQF was adopted to calculate the distribution of the aqueous species (Parkhurst et al., 1996) and mineral saturation states. Thirteen analysts in groundwater from each water samples were used in the calculations. They were pH, E_H, temperature, HCO_3, SO_4, Cl, Ca, Mg, Na, K, As, Fe and Mn.

4. Results and discussion

4.1. Geomorphological classification

The main geological and geomorphological features in the study area are shown in Fig. 1a and b. Based on remote sensing data, field observations and HCA cluster analyses, the study area has been

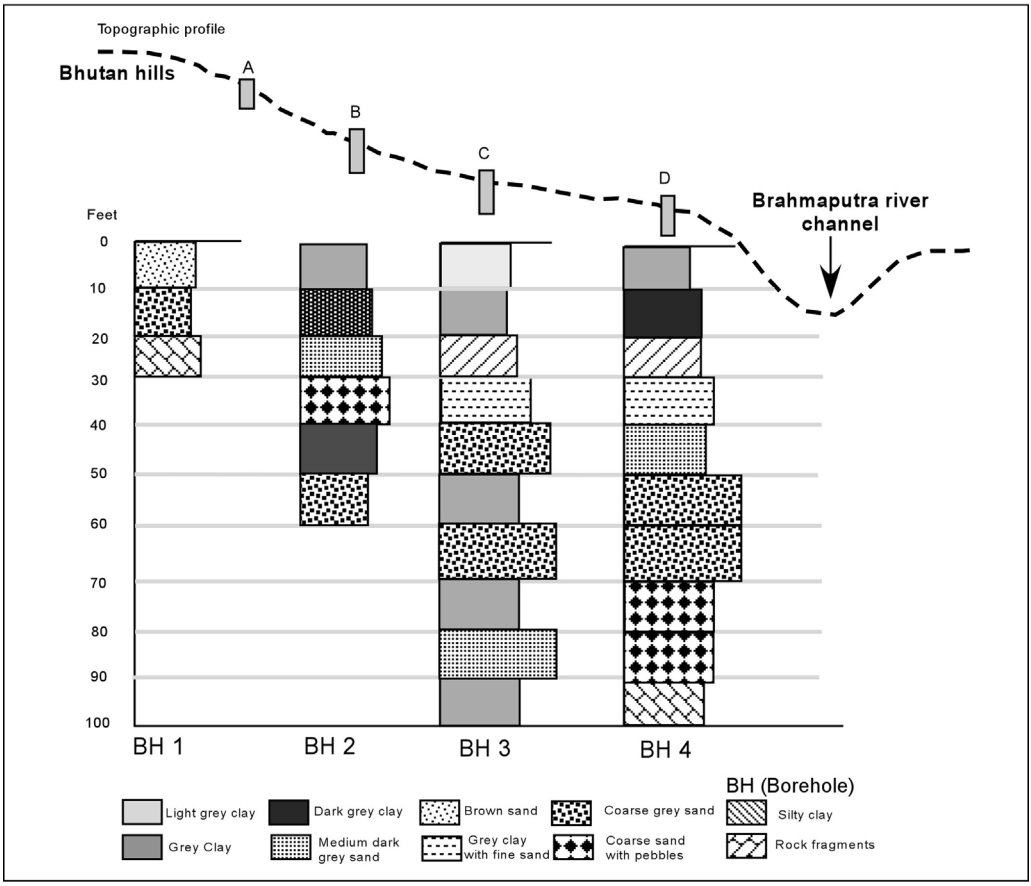

Fig. 2. Lithologs collected from location A, B, C, and D, as indicated in Fig. 1b.

classified in to four different geomorphological units (Fig. 1a and b). These geomorphological units are river channel deposits (RCD), younger alluvial (YA), older alluvial (OA) and piedmont deposits (PD) in the Eastern Himalayan (Bhutan foothills). River channel deposits (RCD) are the braided channel deposits of the Brahmaputra river and are located in the vicinity of the main river channel. Younger alluvial deposits (YA) include the younger and active flood plains, these are generally deposits of the main river channel of Brahmaputra. The older alluvial deposits (OA) comprises the sediments, which were mostly deposited by the northern tributaries of Brahmaputra within the study area draining the Eastern Himalayas in Bhutan and older braided channel of the Brahmaputra river. All of the northern tributaries of Brahmaputra river, within the study area, drain through the Lesser Himalayan rocks and Siwalik Group of Bhutan Himalayas and transport the deposits, forming major parts of the older alluviums. The piedmont deposits (PD) contain very coarse grained sand and debris deposits near the foot hills of Bhutan Himalayas. The subsurface lithologies of all geomorphological terrains are demonstrated by lithologs (Figs. 1b and 2). The depth of the lithologs varies from 6 to 35 m, depending upon the sediments thickness and elevation of terrain. The study area shows high variation in elevation of geomorphic terrains, varying from 130 m (near foothills) to 51 m (main river channel). The sediments of the study area can be derived from two distinct provenances, one is directly from the Bhutan Himalayas and the other through the Tsang Po system of Tibetean Himalayas. The younger alluviam and recently flood sediments are mostly deposited by braided channel of the Brahmaputra, which are brought down from the upstream Tsang Po system of Tibetean Himalayas and/or are derived from reworked sediments of the upper Brahmaputra channel. In the study area, the distance between

Eastern Himalayas (sediments provenance) to main river course of Brahmaputra is very less (~70 km), resulting to high sedimentation rate and immature sediments because of lack of sufficient travel time before reaching the depocenters. According to this observation, groundwater samples collected have been divided into four major terrain groups accordingly, which are viz., River channel deposits (very close to main river channel, $n = 10$ [RCD]); younger alluvium (active and younger flood plains deposits and channel sediments, $n = 37$ [YA]); older alluvial (the older flood plain and interfluve plains, $n = 54$ [OA]), and Piedmont deposits (alluvium and debris deposits in the Bhutan Himalayan foothills, $n = 6$ [PD]).

The HCA analysis resulted into four clusters for the collected groundwater samples (HCA-1 through HCA-4). Cluster 1 and 4 are composed specially of OA and PD. Clusters 2 is generally representing RCD groups (~60%), the YA terrain does not belong to any particular cluster (Fig. 1b).

4.2. Groundwater solute chemistry in different terrains

4.2.1. Major solutes and physical parameters

In the study area, groundwater samples of all different terrains show pH values ranging from (6.8–7.7, median 7.62) indicating circum neutral groundwater (Table 1). Calcium (Ca^{2+}) is the dominant cation in groundwater samples of YA terrain (Table 1), with maximum value of Ca^{2+} for RCD (30.9 mg/L), YA (60.5 mg/L), OA (23.3 mg/L), and PD (6.0 mg/L) respectively. In the older alluvial groundwater samples Na^{+} is the dominant cation, with maximum value (46.6 mg/L). The maximum concentrations of Mg^{2+} are almost similar in RCD and YA whereas the mean concentration of Mg^{2+} is nearly identical in all terrains excluding PD terrain (Table 1). The median concentration of bicarbonate HCO_3^- for RCD (186 mg/L), YA (150 mg/L), OA (119 mg/L), and PD (117 mg/L) values (Table 1). The mean molar ratios of HCO_3^- to total anion concentrations are nearly identical between all terrains except PD. In RCD samples the mean molar concentration ratio of HCO_3^- to total anionic concentrations (0.93), which is very similar to the YA and OA aquifers mean molar ratios of (0.93) and (0.92), respectively but in PD (0.88). In general, indicator of oxidizing conditions like DO (median range 0.26–0.91 mg/L) and NO_3 (median range 1.03–1.39 mg/L), are present in low concentration in all terrains indicating highly reducing condition in study area.

4.2.2. Evaluation of hydrogeochemical facies

The aquifers of four different geomorphic terrains show distinct relationship with major solutes in the groundwater. The Piper plot (Fig. 3) suggests that groundwater of study area can broadly be divided into three hydrogeochemical facies: (1) Ca^{2+}–HCO_3^-; (2) Ca^{2+}–Na^{+}–HCO_3; (3) Na^{+}–Ca^{2+}–HCO_3^-. Previous study (Enmark and Nordborg, 2007) shows almost similar results of groundwater composition in Assam (Darrang). Groundwater of younger alluvium (YA) is predominantly Ca^{2+}–Na^{+}–HCO_3^-, type (~90%) with only few samples belong to Ca^{2+}–HCO_3^- (Fig. 3). The groundwater samples of river channel deposits (RCD) aquifer are mostly Ca^{2+}–HCO_3^- type, whereas the groundwater samples from older alluvium (OA) and piedmont deposits (PD) showed variation between Ca^{2+}–Na^{+}–HCO_3 and Na^{+}–Ca^{2+}–HCO_3^- of hydrogeochemical facies but dominated by Na^{+}–Ca^{2+}–HCO_3^- (~80%). According to previous studies (Zheng et al., 2004; Mukherjee and Fryar, 2008), high HCO_3^- in groundwater of downstream Bengal basin or Central Gangetic plain (Mukherjee et al., 2012), play important roles in hydrochemical evolution and trace metal mobilization. In present study area HCO_3^- gives almost same value for all different alluvial aquifers. Mean groundwater ion composition plotted on Stiff diagram shows that groundwater of RCD and YA terrains are dominated by Ca^{2+} cation. The groundwater composition of OA and PD terrains are almost similar dominated by $Na^{+} + K^{+}$ cations (Fig. 4).

4.2.3. Chemical evolution of groundwater

Hydrogeochemical evolution of groundwater depends on the chemistry of recharging water, water–aquifer matrix interaction (e.g. cation exchange), or both, as well as groundwater residence time within the aquifers (Drever, 1997). There are three general processes by which major solutes are mostly introduced to groundwater from the aquifer matrix: evaporite dissolution, carbonate dissolution, and silicate weathering (Garrels and MacKenzie, 1971; Mukherjee et al., 2010). The rate of weathering is also an important factor in the chemical evolution of groundwater. According to

Table 1
Statistical summary of selected parameters, solutes and stable isotope compositions of the groundwater for each of the terrain in the study area. Below detection level concentrations are marked as bdl.

		RCD ($n=10$)				YA ($n=37$)				OA ($n=54$)				PD ($n=6$)			
		Min	Max	Mean	Median	Min	Max	Mean	Median	Min	Max	Mean	Median	Min	Max	Mean	Median
Depth	m	14	46	36	32	6	40	33	37	5	59	28	38	3	8	5	5
Temp	(°C)	25	26.4	25.5	25.2	23.3	29.5	25.2	26.3	23.9	26.8	24.8	24.5	24.3	26.6	25.1	25.5
E_H	mV	28	54	41	36	32	162	51	32	38	198	86	50	109	169	135	116
pH		6.77	7.71	7.17	7.60	6.08	7.63	6.84	7.34	6.14	7.80	6.83	7.55	7.21	7.70	7.47	7.52
DO	mg/L	0.25	2.72	0.92	0.61	0.21	1.94	0.64	0.23	0.20	1.92	0.62	0.91	0.13	1.60	0.89	0.28
SC	μS	93	231	170.5	210	58	324	174	172	111	385	196	189	78	241	160	191
Na	mg/L	6.2	23.3	12.1	21.5	5.1	23.5	11.5	14.9	4.9	46.6	17.7	22.5	5.5	13.5	9.3	9.2
Mg	mg/L	2.6	14.9	8.2	12.2	1.5	17.8	7.7	7.5	2.4	16.2	6.4	6.5	3.7	6.4	4.8	5.6
Ca	mg/L	12.9	30.9	20.1	22.6	5.7	60.5	15.4	18.0	4.1	23.3	10.8	12.6	3.2	5.9	4.3	4.1
K	mg/L	1.8	9.5	4.1	1.9	1.0	5.9	2.8	1.4	1.1	19.8	3.3	1.5	2.1	6.3	4.6	6.0
Fe	mg/L	0.65	19.39	5.68	1.82	1.11	28.80	12.68	1.26	1.11	41.02	18.66	17.67	2.55	36.92	17.83	16.23
Mn	mg/L	0.20	2.24	0.91	0.68	0.21	5.87	1.30	0.24	0.29	2.45	1.10	0.62	0.05	1.16	0.63	0.59
As	mg/L	bdl	0.06	0.02	bdl	bdl	0.05	0.01	bdl	bdl	0.13	0.03	0.04	bdl	0.04	0.01	0.02
HCO_3^-	mg/L	113	201	142	187	63	242	129	150	70	269	138	139	90	150	126	117
SO_4^-	mg/L	0.7	16.6	4.9	3.6	0.9	14.2	3.9	8.9	0.1	11.5	3.0	2.9	0.9	20.1	7.2	1.3
Cl^-	mg/L	2.1	12.7	4.2	3.1	1.0	10.0	3.9	4.8	0.9	30.9	5.1	2.1	1.8	10.4	6.6	7.0
NO_3^-	mg/L	1.10	3.18	1.65	1.39	1.15	31.02	2.93	1.22	0.28	6.52	1.96	1.29	0.45	7.57	2.39	1.03
F	mg/L	0.29	1.02	0.52	0.31	0.30	1.00	0.52	0.36	0.20	1.19	0.64	0.90	0.21	1.94	0.76	1.20
$\delta^{18}O$	per mil	–	–	–	–	−7.66	−2.69	−4.74	−7.19	−6.87	−3.20	−4.51	−4.73	−6.77	−3.79	−5.54	−4.87
$\delta^{2}H$	per mil	–	–	–	–	−49.10	−12.70	−28.75	−46.11	−44.10	−18.32	−28.02	−29.60	−45.22	−23.17	−36.38	−30.63

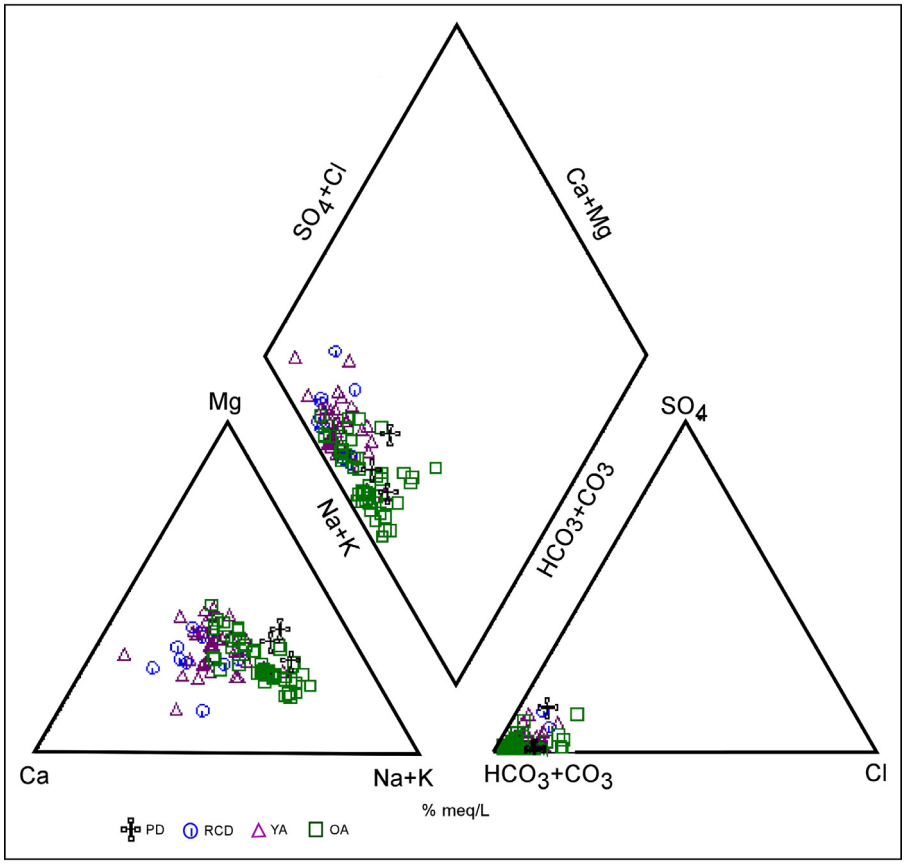

Fig. 3. Piper Plots of groundwater samples collected from the study area (RCD, River channel deposits; YA, Younger alluviums; OA, Older alluviums; PD, Piedmont deposits).

Meybeck (1987), weathering rates of carbonates are up to ~12 times faster than silicate weathering rate. Therefore, groundwater chemistry can be significantly influenced by the presence of more leachable lithotypes, as well as their residence time.

To estimate the sources of the major ions in the groundwater of different alluvial terrains of the study area, bivariate plots and molar ratios are used in this study. The bivariate mixing plots (Fig. 5) of Na-normalized Ca versus Na-normalized Mg and Na-normalized HCO_3^-, examine the relative contribution of three major weathering mechanisms (silicate, carbonate, and evaporate) to solute concentration in groundwater (Gaillardet et al., 1999; Mukherjee and Fryar, 2008; Mukherjee et al., 2012). Bivariate plots show that most of the groundwater samples of older alluvium (OA) and all samples of piedmont deposits (PD) terrain are within or very close to global-average silicate weathering domain and some of the YA groundwater samples are plotted toward carbonate dissolution zone (Fig. 5). However, the groundwater composition of RCD and YA terrain are transitional between the global-average carbonate dissolution and silicate weathering zones. The ratios of Ca + Mg to total cations are almost equal for the groundwater samples of RCD and YA terrains (mean ratio 0.57 for RCD and 0.54 for YA) and higher than OA and PD groups (mean ratio 0.39 for OA; 0.38 for PD) (Fig. 6a). In the same way, the ratio of Na + K to total cations tends to be high for groundwater samples of OA and PD terrains (mean ratio = 0.61, 0.62 respectively), low for RCD (mean ratio is 0.43) and YA (mean ratio is 0.46). According to these plots (Fig. 6a), Ca^{2+} and Mg^{2+} are dominant cation in RCD and YA groundwater samples which can be derived from silicate (Ca-feldspar) and carbonate (calcite and

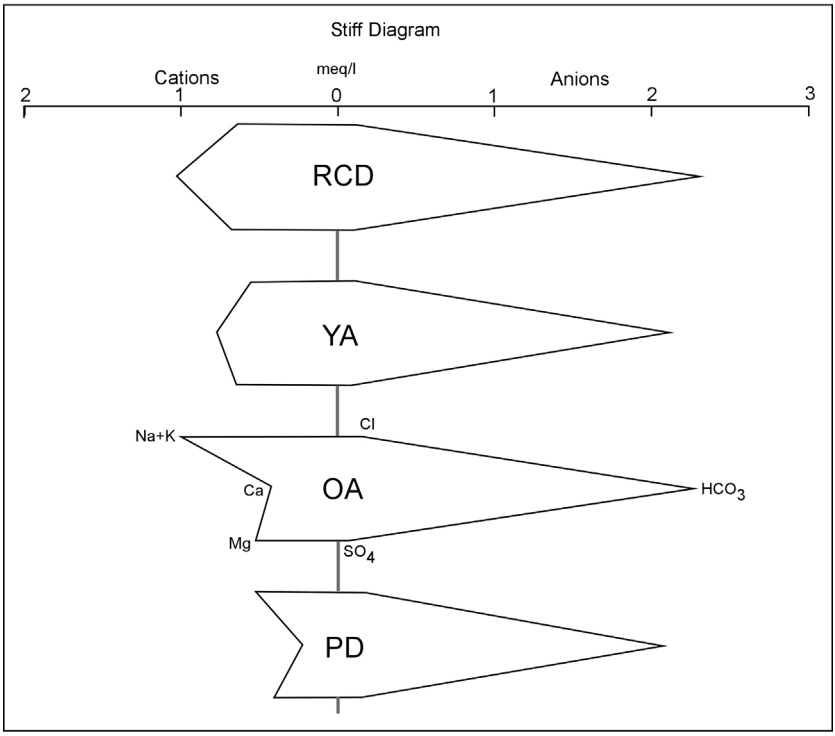

Fig. 4. Stiff diagram of mean groundwater compositions observed in the study area, classified by terrain types (YA, Younger alluvium; OA, Older alluvium; PD, Piedmont deposits).

dolomite) weathering whereas the predominance of Na^+ and K^+ in OA and PD, derived from silicate weathering probably due to dissolution of orthoclase, mica and pyroxene minerals derived from the Siwalik sediments and meta-sediments derived from the Himalayan metamorphic terrains.

Most of the groundwater samples, especially of OA terrain tend to fall along the 1:2 line on bivariate plot of HCO_3^- versus Na + K and samples that fall below the 1:1 line on bivariate plot of Na + K versus total cation suggest that silicate weathering as a dominant process to introduce major ion in groundwater of all alluvial terrains (Fig. 6b). In the cation exchange reaction, the bivalent cations (Ca^{2+} and Mg^{2+}) are exchanged by mono-valent cations (Na^+ and K^+) from the aquifer matrix to groundwater. Bivariate plot (Fig. 7) shows the influence of cation exchange, where the trend line with slope ~−1, i.e. indicates that cation exchange probably has strong influence on the water chemistry of aquifers. According to Fig. 7, groundwater samples collected from all alluvial terrain (RCD, YA, OA and PD) have no inclination toward the $y = -x$ line, and ploted very close to origin (range between −0.16 to −0.3), suggesting that cation exchange probably has no influence on the groundwater chemistry of the study area. This might be a reflection of the shorter groundwater residence time and immature sediments because the distance between the source (Eastern Himalayas) and depocenters of the studied aquifers are very less (~70 km), in contrast to the Bengal basin of Ganges system, which demonstrate longer flow paths leading to significant cation exchange reactions between aquifer matrix and ambient groundwater. On the basis of this observation, mineral weathering is deduced to be the dominant mechanism in evolution of cations in the groundwater of study area.

4.2.4. Redox environment

Groundwater samples collected from the four different geomorphic terrains indicate highly reducing conditions in the study area (Fig. 8). Very low concentrations of dissolved O_2 were detected in

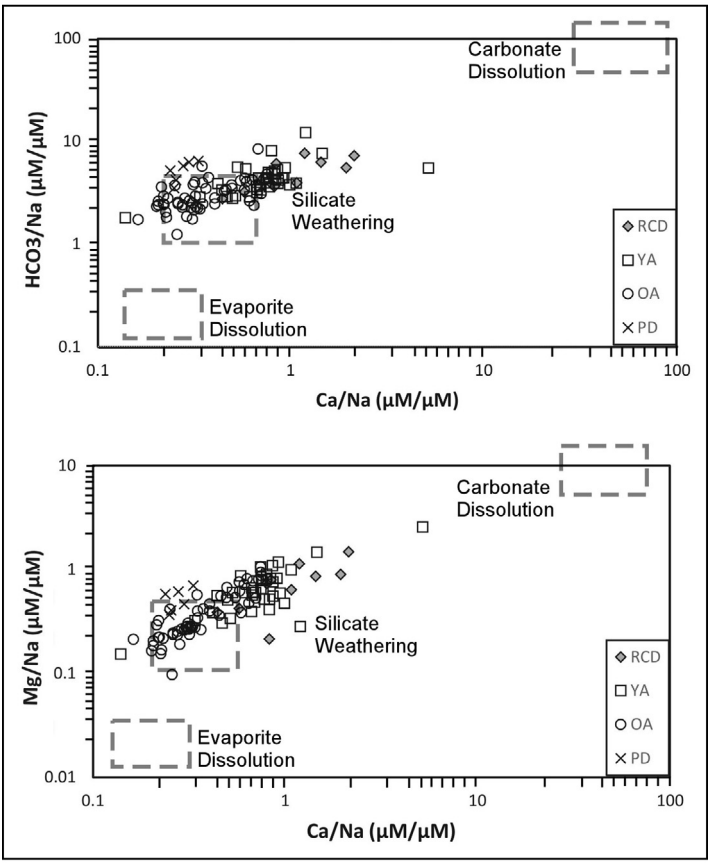

Fig. 5. Bivariate plots of Na-normalized (μM/μM) Mg versus Ca and HCO_3 versus Ca to show trends of weathering. The dashed rectangular areas demonstrate global average compositions of groundwater with respect to evaporite dissolution, silicate weathering, and carbonate dissolution without mixing (following Gaillardet et al., 1999 and Mukherjee et al., 2012).

groundwater of all alluvial terrains i.e. (for RCD mean: 0.92 mg/L, YA mean: 0.64 mg/L, OA mean: 0.62 mg/L and PD mean: 0.89 mg/L) (Table 1) with the mean concentrations being less than 1 mg/L. The E_H values are generally low (ranges +28 mV to +198 mV) in different alluvial terrains (Table 1). The measured E_H values, which typically represent a composite of multiple redox-sensitive solutes (Langmuir, 1971; Postma and Jakobsen, 1996; Mukherjee et al., 2008) were converted to pe (where pe = 16.9 E_H at 25 °C) and plotted against the equilibrium pe (at temperature similar to sampled groundwater temperature) of different redox couples. The values of pe for all terrains ranged between (median ranges 0.5–1.95). Samples from RCD site showed very low range of pe values and fall around As (V) reduction zone (mean, pe = 0.76). However, OA terrain has wider range of pe values (0.6-3.34; mean 1.5) than those of the YA terrain (0.5-2.7; mean 0.8) and PD terrain (1.8-2.9; mean 2.3). Therefore the groundwater samples of different alluvial terrains fall in the postoxic subgroup of anoxic environment and the mean pe values are lower than Fe (III) reduction and very close to As (V) reduction (Fig. 8). Thus, a resultant metal-reducing condition, with As-liberation appears to be the dominant redox environment in the study area.

4.3. Recharge to aquifers

The range of $\delta^{18}O$ and $\delta^{2}H$ values as achieved from groundwater samples of study area are showing in Fig. 9a, can be noted between the three areas: the PD samples ($\delta^{18}O$ range ~−4‰ to −7‰ VSMOW),

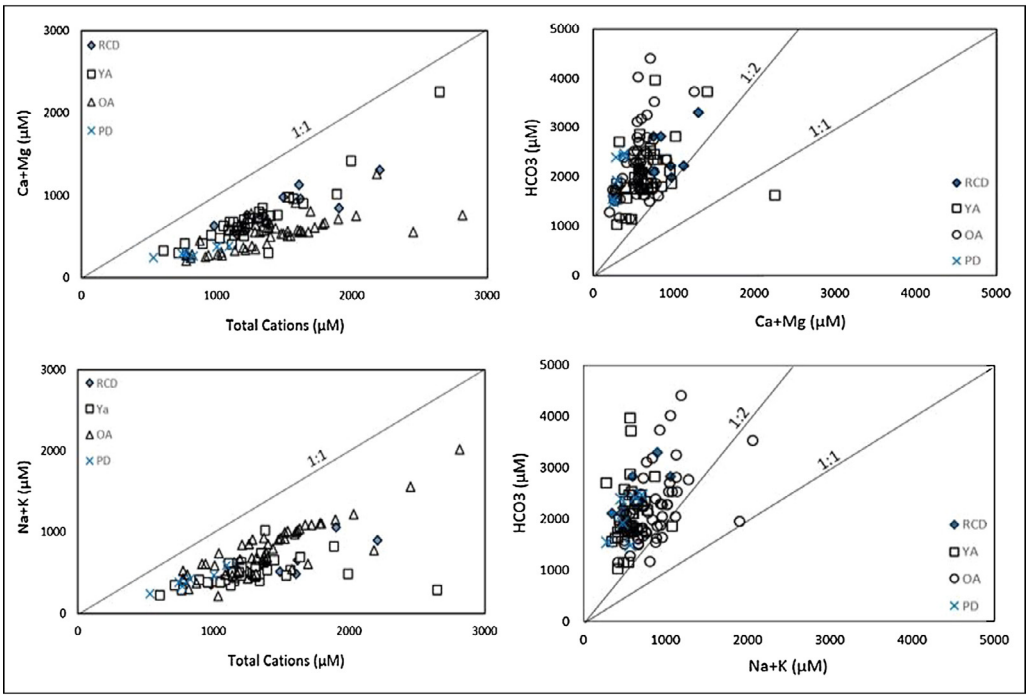

Fig. 6. (a) Bivariate plots of Ca + Mg and Na + K versus total cation concentration in the groundwater samples; (b) Bivariate plots of HCO_3 versus Ca + Mg and Na + K in the groundwater samples (RCD, River channel deposits; YA, Younger alluvium; OA, Older alluvium; PD, Piedmont deposits).

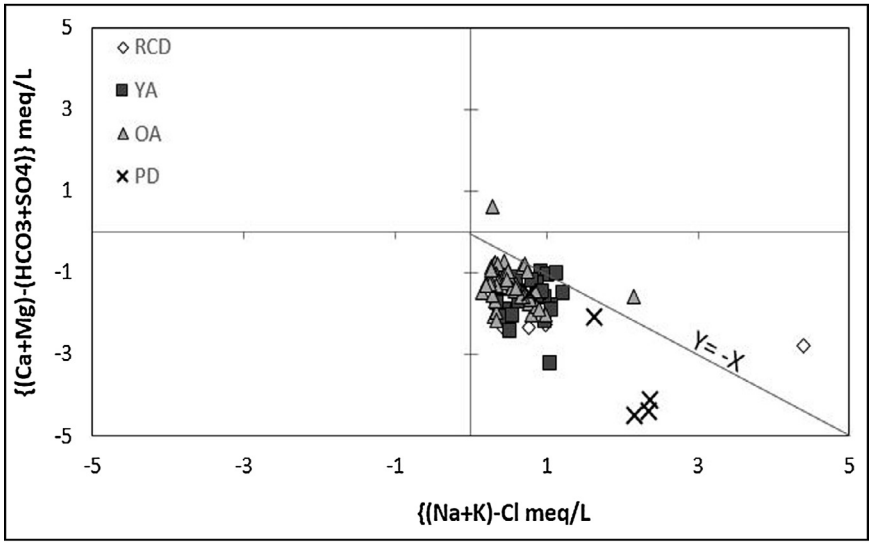

Fig. 7. Bivariate plot of (Ca and Mg) less (HCO_3^- and SO_4^{2-}) against Na and K less Cl to indicate the cation exchange reactions (RCD, River channel deposits; YA, Younger alluvium; OA, Older alluvium; PD, Piedmont deposits).

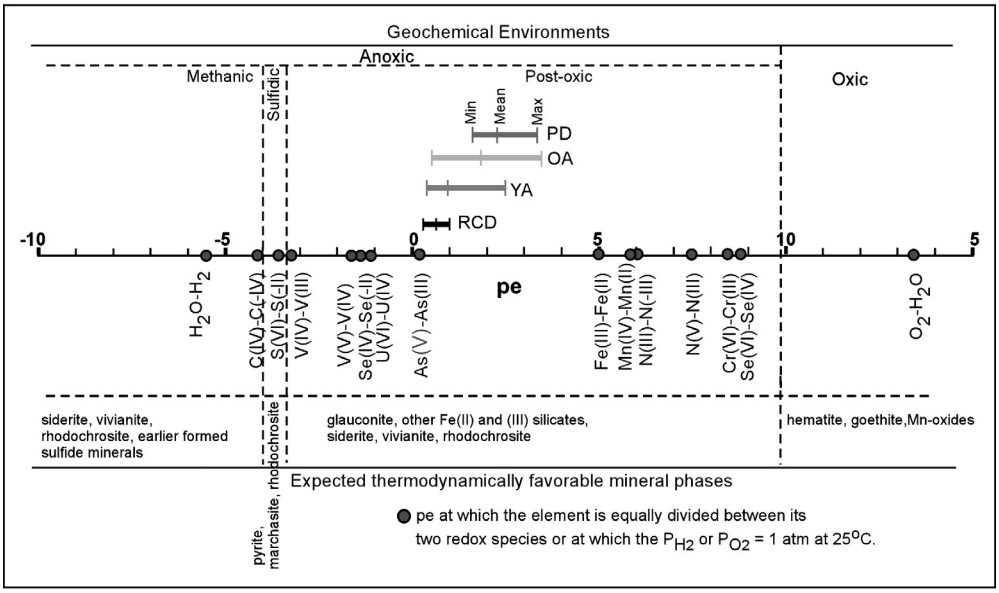

Fig. 8. Plot shows ranges of pe values observed in groundwater samples (converted from measured E_H values) of the samples collected from the study area in comparison to the equilibrium pe values of common redox couples generally observed in groundwater. The plot also demonstrates the geochemical environment and the thermodynamically favorable mineral phases expected in groundwater in respect to the redox species (RCD, River channel deposits; YA, Younger alluvium; and OA, Older alluvium; PD, Piedmont deposits) [after Mukherjee et al. (2008)].

OA ($\delta^{18}O$ range ~−3‰ to −7‰ VSMOW) and YA samples ($\delta^{18}O$ range ~−3‰ to −8 ‰ VSMOW). Likewise, the δ^2H range for the PD (~−23 ‰ to ~−45 ‰ VSMOW), for OA samples (~−18 ‰ to ~−44‰ VSMOW) and for YA samples (~−12 ‰ to ~−50 ‰ VSMOW) (Table 1). Assuming that at least the shallow aquifers (<60 m) in study areas were recharged under present-day climatic conditions that may be explained by several mechanisms: present day rainfall, surface water infiltration, and horizontal groundwater inflow from rivers. According to this observation, the groundwater samples of all alluvial terrains fall along the Global Meteoric Water Line (GMWL: $\delta^2H = 8\ \delta^{18}O + 10$) of Craig (1961). The trend for PD, OA and YA samples ($\delta^2H = 7.3\ \delta^{18}O + 4.3$; $\delta^2H = 7.1\ \delta^{18}O + 5$; and $\delta^2H = 6.8\ \delta^{18}O + 2.7$ respectively), which is sub parallel to the GMWL, suggest that some evaporation may have taken place through recharging water in study area. Fig. 9b shows that no consistent variation in $\delta^{18}O$ with latitude is observed within the groundwater samples from the study area, because the distance between geomorphic terrains is very less (e.g. distance between PD to RCD is <60 km). This is not sufficient for isotopic variation with latitude. Hence the groundwater compositions in shallow aquifers of these geomorphic terrains are influenced by evaporation and other mechanism as already proposed.

4.4. Geochemical modeling

Saturation index calculations for groundwater of all geomorphologic terrains were carried out to calculate saturated and undersaturated mineral phase. Table 2 lists the ranges of SI values for some of the important phases that are thought to affect the chemistry of the groundwater of different geomorphic terrains in the study area. The groundwater is generally highly undersaturated with respect to O_2 and has higher CO_2 than the atmosphere, suggests a strong input of CO_2 from the degradation of organic matter. The groundwater of study area are highly undersaturated with respect to the major As phases (e.g. arsenolite, As_2O_5, and $FeAsO_4{\cdot}2H_2O$) and Mn oxide phases (e.g. birnessite, bixbyite, manganite, and pyrolusite), representing that when As and Mn enter into solution, they do not precipitate as those phases. In the study area, groundwater is supersaturated with respect to Fe (III) (oxyhydr)oxide phases like magnetite, hematite, goethite, in RCD and YA terrains while highly supersaturated in OA

Table 2
Summary of saturation indices (SI) calculated by PHREEQC for some mineral phases possibly in groundwater of all geomorphic terrains.

Phase name	Formula	RCD ($n=10$)			YA ($n=37$)			OA ($n=54$)			PD ($n=6$)		
		Mean	Max	Min	Mean	Max	Min	Mean	Max	Min	Mean	Max	Min
Arsenolite	As_4O_6	−14.53	−13.43	−15.64	−13.74	−11.28	−18.61	−15.88	−11.46	−28.06	−23.32	−21.51	−25.16
	As_2O_5	−31.35	−30.9	−31.86	−31.67	−30.15	−34.02	−31.22	−28.88	−33.98	−33.08	−32.59	−33.38
Birnessite	MnO_2	−18.52	−16.59	−20.08	−19.51	−17.25	−22.20	−18.33	−11.92	−21.85	−14.49	−13.18	−15.6
Bixbyite	Mn_2O_3	−16.01	−13.19	−18.7	−17.63	−14.19	−21.69	−16.45	−8.25	−20.96	−11.68	−9.81	−13.15
Calcite	$CaCO_3$	−0.72	0.1	−1.24	−1.24	−0.25	−2.47	−1.38	−0.51	−2.04	−1.13	−0.69	−1.52
	Log Pco_2	−1.96	−1.58	−2.41	−1.72	−1.02	−3.7	−1.65	−0.8	−2.77	−2.30	−2.19	−2.48
Dolomite	$CaMg(CO_3)_2$	−1.47	0.3	−2.94	−2.42	−0.44	−4.81	−1.87	−1.04	−2.76	−2.64	−1.02	−4.08
Goethite	FeOOH	5.89	7.02	5.07	5.33	7.02	3.26	6.14	9.69	2.66	8.69	9.69	8.26
Gypsum	$CaSO_4{\cdot}2H_2O$	−3.54	−2.61	−4.2	−3.5	−1.18	−4.14	−3.92	−3.21	−5.03	−4.17	−3.29	−4.73
Hematite	Fe_2O_3	13.79	16.06	12.05	12.68	16.1	8.52	14.3	21.4	7.33	19.41	21.39	18.52
Hausmannite	Mn_3O_4	−17.37	−13.62	−21.14	−19.52	−14.94	−24.93	−18.48	−8.39	−24.02	−12.68	−9.93	−15.24
Magnetite	Fe_3O_4	16.02	18.95	13.67	14.59	19.37	8.84	16.44	25.02	7.36	22.63	25.55	20.96
Manganite	MnOOH	−8.18	−6.74	−9.49	−9.20	−7.22	−18.58	−8.35	−4.26	−10.63	−5.98	−5.11	−6.65
	Log Po_2	−51.32	−49.53	−52.49	−52.39	−47.51	−55.5	−50.12	−40.81	−55.62	−44.16	−41.95	−45.96
Pyrolusite	MnO_2	−16.22	−14.36	−17.85	−17.28	−15.05	−20.09	−16.14	−9.71	−19.66	−12.26	−11.06	−13.39
Rhodocrosite	$MnCO_3$	0.34	1.06	−0.46	0.03	0.98	−0.74	0.04	1.04	−0.65	0.52	1.57	−0.77
Scorodite	$FeAsO_4{\cdot}2H_2O$	−7.56	−7.28	−8.05	−8.34	−6.6	−10.62	−7.30	−4.43	−11.63	−5.56	−4.61	−6.06
Siderite	$FeCO_3$	0.70	1.07	0.15	0.72	1.6	−0.4	0.98	1.88	−0.67	1.16	2.13	0.17

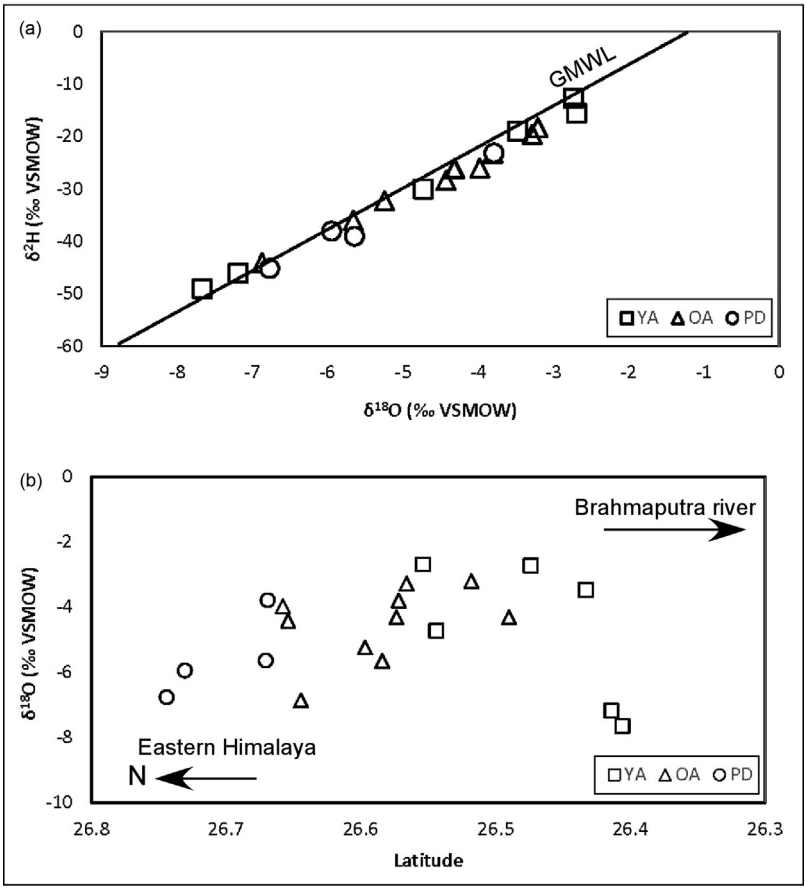

Fig. 9. (a) Bivariate plot of $\delta^{18}O$ and $\delta^{2}H$. The Global Meteoric Water Line (GMWL) of Craig (1961) is provided for reference; (b) Plot of $\delta^{18}O$ with latitude observed in the study area, classified by terrain types (YA, Younger alluvium; OA, Older alluvium; PD, Piedmont deposits).

and PD, indicating that precipitation of Fe(III) phases from groundwater is thermodynamically favorable. In all the four geomorphic terrains, groundwater samples were under saturated with respect to carbonate phases such as calcite ($CaCO_3$) and dolomite ($MgCa(CO_3)_2$) and generally give the similar values (mean) among these units. This is in a good agreement with higher concentration of Ca, Mg and bicarbonate in the groundwater samples. Groundwater is slightly supersaturated with respect to rhodochrosite ($MnCO_3$) and siderite ($FeCO_3$). The saturation states of Fe- and Mn-bearing carbonates, and oxides in the groundwater indicate favorable conditions for potential As adsorption onto the surfaces of Fe- and Mn-bearing oxides and carbonates formed under oxidizing and reducing conditions, respectively.

4.5. Groundwater arsenic

4.5.1. Distribution in different geomorphic terrains

Approximately ~65% of groundwater samples collected from the study area are enriched with dissolved As concentrations >0.01 mg/L (0.01 mg/L; WHO standard for safe drinking water), and it range from <0.001 to 0.13 mg/L (mean 0.025 mg/L) for all groundwater samples combined. According to previous study (Enmark and Nordborg, 2007), the highest concentration of As in aquifers of northwestern parts of Brahmaputra River basin is recorded as 0.06 mg/L which is quite low in comparison

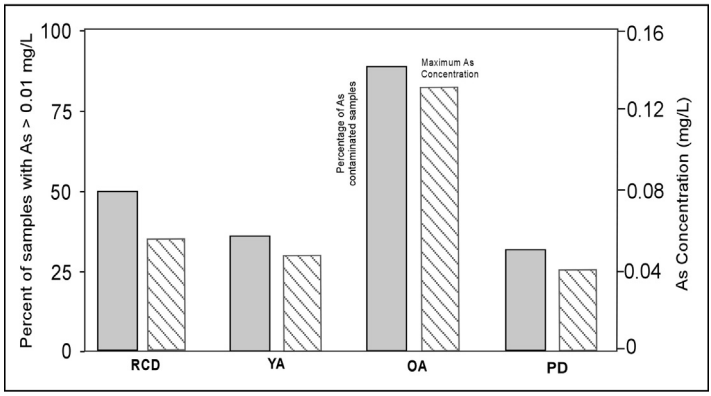

Fig. 10. Plot showing percentage of groundwater samples in each terrain that have As concentrations >0.01 mg/L, along with the maximum concentration of As in the groundwater samples from the respective terrains (RCD, YA, OA and PD).

with present study. Terrain classification of study area showed that more than 85% groundwater samples of OA, ~50% of RCD, ~35% of YA and ~33% of PD terrain, have dissolved As concentration >0.01 mg/L (Fig. 10). The discussion so far has shown that hydrogeochemical condition of the study area is influenced by geomorphologic disposition of the aquifers. The groundwater As concentrations show interesting patterns among the four terrains. It is highest in the aquifers of OA terrain, ranging from (<0.001–0.13 mg/L, median 0.072), whereas aquifers of PD terrain are least As (<0.001–0.04 mg/L, median 0.01) enriched. Groundwater samples of RCD and YA terrains are less contaminated, where dissolved As concentrations ranges from (<0.001–0.06 mg/L, median 0.01) and (<0.001–0.05 mg/L, median 0.005) respectively. Previous studies (e.g. Chatterjee et al., 2010; Mukherjee et al., 2011, 2012), suggested that recent Ganges fluvial sediments (YA) are highly enriched by As, whereas OA samples are least As contaminated (Bengal basin and Central Gangetic plains) in India and Bangladesh. In case of the Brahmaputra basin (present study), OA aquifers appear to be more enriched by As in groundwater in comparison to other terrains, and aquifers of YA terrain are less contaminated, which is contrary from previous studies. This difference may be related to palaeogeomrphology and hydrology, present-day river channel morphology and sediments transportation rates. In the study area, the higher flushing rate of sediments, caused by river channel (braided for Brahmaputra river, in contrast to meandering in Ganges river) and high gradient (steep slope), along with aquifer sediment provenance and sediment immaturity due to small distance between sediment source and depo-center (~70 km) may have together attributed to this discernable difference. In the present study, all the collected groundwater samples are of shallow depths. Hence no variation in vertical distribution of As was observed (Fig. 11). Therefore, among all the shallow water wells, depth is not a controlling factor in the distribution of As in different geomorphologic terrains.

Recent studies on provenance of groundwater As in the Himalayas (e.g. Saunders et al., 2005; Stanger, 2005; Guillot and Charlet, 2007; Mukherjee et al., 2014) suggested that Siwalik Group, which acts as the immediate provenance of the Himalayas sediments, is the probable reservoir of As and the As-enriched consolidated and unconsolidated lithologies are more dominant in the palaeo-forelands (e.g. Siwaliks) of the Himalayan orogen, than the medium to high-grade metasediments in the Higher Himalayas. Moreover, the evolution of palaeogeomorphology and hydrogeological setup may also have influenced the groundwater chemistry of Brahmaputra. The migration pattern of the Brahmaputra River through ages has been quite drastic and has resulted through a complex tectono-geomorphic evolution (Lang and Huntington, 2014; Coleman, 1969). Several authors (e.g. Guillot and Charlet, 2007; Stanger, 2005; Mukherjee et al., 2014) have suggested that during the Miocene, the major (proto)-Himalayan rivers probably flowed directly from the southern Tibetan plateau to the foreland basin leading to important weathering of the Indus-Tsangpo suture zone, transport of As and other solutes and their sink in the Siwalik foreland basin. After 5 Ma to present, the Siwalik was strongly uplifted and eroded, due to the activation of the Main Frontal Thrust (MFT) and the landscape underwent reshaping due to major tectonic movements and sudden and drastic changes in the climate conditions.

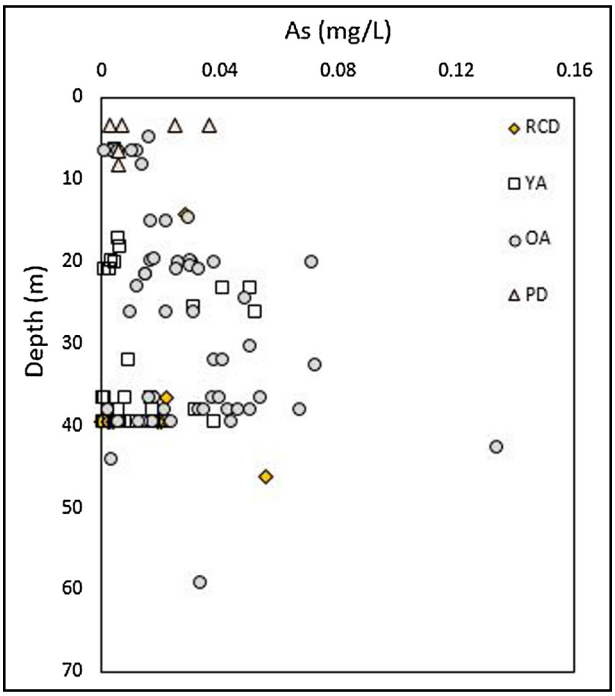

Fig. 11. Plots showing relationship between As and groundwater well depths of different alluvial terrains (RCD, YA, OA and PD).

The combination of strong tectonic activities and a wetter climate during the Holocene lead to the removal of these solutes stored in the Siwalik sediments.

Thus, this knowledge can be translated to the fact that the Siwalik deposits located in the Bhutan foothills, due north of the study area and that act as the sediments to the OA aquifers through multiple lower-order tributaries of the Brahmaputra, should be a more acute source of solid-phase As accumulating in the aquifers, than the sediments that can be dominantly sourced to the Higher Himalayas and Tibetian highlands, and are recently deposited by the Brahmaputra. However, the reason that groundwater of all aquifers are As enriched to certain extent are related to the fact that during higher stage of the Brahmaputra, much of the sediments from various provenances are reworked, adulterated, mixed and re-deposited that eventually become part of the original aquifers.

4.5.2. Relationship with other solutes

The groundwater samples collected from the four geomorphic terrains showed a distinct relationship of As with several other groundwater solutes. To calculate the relation of As with other hydrochemical parameters, nonparametric correlation analyses of Spearman's rho (ρ) was calculated (Table 3). This correlation suggested that in the present study area different geochemical processes control As mobilization in different terrains. Numerous studies in the downstream and adjoining Bengal basin have previously described the relationships of As with other solutes (e.g. Bhattacharya et al., 1997; Ravenscroft et al., 2001; Zheng et al., 2004; Biswas et al., 2011) and combined effects of HCO_3^- and pH in As mobilization from surface of Fe–Mn(OOH) and aquifer sediments (Anawar et al., 2003). One of the main discussion has been about the reduction of different metal(loid)s (Bhattacharya et al., 1997; Islam et al., 2004) and As resorption to residual (oxyhydr) oxides. The supersaturation of metal oxides and hydroxides can be affect As resorption process as detected in Gangetic basin (e.g. Mukherjee and Fryar, 2008). Lot of discussions have been about the relationship between Fe and As. While, many studies showed very close positive co-relationship (e.g. Bhattacharya et al., 1997; Dowling et al., 2002; Stüben et al., 2003, etc.), many studies noted correlations between As and other

Table 3
Results of nonparametric Spearman rho calculation, classified by terrain. Rho for arsenic, where available, is marked in bold.

	E_H	DO	SC	pH	Na	K	Ca	Mg	Cl	HCO_3	SO_4	NO_3	Fe	Mn	As	F
RCD group																
E_H	1.00	−0.22	0.08	−0.92	−0.22	0.73	0.04	−0.38	−0.07	−0.32	−0.56	−0.02	0.56	−0.03	0.24	0.19
DO	−0.22	1.00	0.02	0.27	0.07	0.03	0.15	0.30	0.46	0.17	0.73	−0.16	−0.37	0.27	0.24	−0.25
SC	0.08	0.02	1.00	0.15	0.39	−0.20	0.46	0.21	0.56	0.33	0.07	−0.14	−0.58	−0.29	−0.21	−0.44
pH	−0.92	0.27	0.15	1.00	0.25	−0.67	0.18	0.65	0.16	0.53	0.62	0.10	−0.64	0.01	−0.27	−0.41
Na	−0.22	0.07	0.39	0.25	1.00	−0.71	0.08	0.15	−0.10	0.42	−0.09	−0.71	−0.31	0.01	−0.50	−0.67
K	0.73	0.03	−0.20	−0.67	−0.71	1.00	−0.03	−0.12	0.15	−0.34	−0.12	0.39	0.46	−0.09	0.33	0.46
Ca	0.04	0.15	0.46	0.18	0.08	−0.03	1.00	0.48	0.09	0.40	0.08	−0.24	−0.35	0.58	0.35	−0.64
Mg	−0.38	0.30	0.21	0.65	0.15	−0.12	0.48	1.00	0.21	0.73	0.48	0.16	−0.46	0.03	−0.31	−0.61
Cl	−0.07	0.46	0.56	0.16	−0.10	0.15	0.09	0.21	1.00	0.20	0.53	0.36	−0.67	−0.46	−0.13	0.02
HCO_3	−0.32	0.17	0.33	0.53	0.42	−0.34	0.40	0.73	0.20	1.00	0.48	−0.09	−0.66	−0.12	−0.60	−0.83
SO_4	−0.56	0.73	0.07	0.62	−0.09	−0.12	0.08	0.48	0.53	0.48	1.00	0.14	−0.69	−0.09	−0.13	−0.25
NO_3	−0.02	−0.16	−0.14	0.10	−0.71	0.39	−0.24	0.16	0.36	−0.09	0.14	1.00	0.04	−0.44	−0.01	0.52
Fe	0.56	−0.37	−0.58	−0.64	−0.31	0.46	−0.35	−0.46	−0.67	−0.66	−0.69	0.04	1.00	0.21	0.37	0.50
Mn	−0.03	0.27	−0.29	0.01	0.01	−0.09	0.58	0.03	−0.46	−0.12	−0.09	−0.44	0.21	1.00	0.72	−0.27
As	**0.24**	**0.24**	**−0.21**	**−0.27**	**−0.50**	**0.33**	**0.35**	**−0.31**	**−0.13**	**−0.60**	**−0.13**	**−0.01**	**0.37**	**0.72**	**1.00**	**0.31**
F	0.19	−0.25	−0.44	−0.41	−0.67	0.46	−0.64	−0.61	0.02	−0.83	−0.25	0.52	0.50	−0.27	0.31	1.00
YA group																
E_H	1.00	0.39	0.17	−0.63	−0.19	0.43	−0.22	0.20	0.20	−0.19	−0.29	0.03	0.60	0.54	0.38	0.02
DO	0.39	1.00	0.14	-0.02	0.03	−0.02	0.00	0.15	−0.09	0.09	0.16	−0.03	0.27	0.25	0.34	0.27
SC	0.17	0.14	1.00	−0.04	0.07	0.27	0.46	0.67	0.34	0.30	−0.06	−0.07	0.34	0.31	0.46	0.11
pH	−0.63	−0.02	−0.04	1.00	0.47	−0.48	0.35	−0.04	−0.09	0.47	0.05	−0.24	−0.51	−0.73	−0.26	0.12
Na	-0.19	0.03	0.07	0.47	1.00	−0.26	0.24	0.04	−0.02	0.46	0.00	−0.06	−0.17	−0.38	−0.08	0.14
K	0.43	−0.02	0.27	−0.48	−0.26	1.00	−0.16	0.25	0.17	−0.33	−0.26	0.21	0.56	0.54	0.40	−0.12
Ca	−0.22	0.00	0.46	0.35	0.24	−0.16	1.00	0.62	0.22	0.48	−0.15	−0.22	−0.18	−0.07	0.01	−0.05
Mg	0.20	0.15	0.67	−0.04	0.04	0.25	0.62	1.00	0.20	0.21	−0.28	0.02	0.29	0.42	0.35	−0.02
Cl	0.20	−0.09	0.34	−0.09	−0.02	0.17	0.22	0.20	1.00	0.16	0.21	0.04	0.04	0.04	−0.09	0.00
HCO_3	−0.19	0.09	0.30	0.47	0.46	−0.33	0.48	0.21	0.16	1.00	−0.03	−0.10	−0.17	−0.30	−0.08	0.25
SO_4	−0.29	0.16	−0.06	0.05	0.00	−0.26	−0.15	−0.28	0.21	−0.03	1.00	−0.07	−0.17	−0.14	−0.15	0.08
NO_3	0.03	−0.03	−0.07	−0.24	−0.06	0.21	−0.22	0.02	0.04	−0.10	−0.07	1.00	0.17	0.27	0.15	0.08
Fe	0.60	0.27	0.34	−0.51	−0.17	0.56	−0.18	0.29	0.04	−0.17	−0.17	0.17	1.00	0.51	0.54	0.17
Mn	0.54	0.25	0.31	−0.73	−0.38	0.54	−0.07	0.42	0.04	−0.30	−0.14	0.27	0.51	1.00	0.54	0.17
As	**0.38**	**0.34**	**0.46**	**−0.26**	**−0.08**	**0.40**	**0.01**	**0.35**	**−0.09**	**−0.08**	**−0.15**	**0.15**	**0.54**	**0.54**	**1.00**	**0.48**
F	0.02	0.27	0.11	0.12	0.14	−0.12	−0.05	−0.02	0.00	0.25	0.08	0.08	0.17	0.17	0.47	1.00

Table 3 (*Continued*)

	E_H	DO	SC	pH	Na	K	Ca	Mg	Cl	HCO_3	SO_4	NO_3	Fe	Mn	As	F
OA group																
E_H	1.00	−0.08	−0.03	0.30	−0.25	0.35	−0.58	−0.57	0.56	−0.35	−0.16	−0.46	0.29	−0.16	−0.51	−0.39
DO	−0.08	1.00	0.21	0.04	0.36	−0.24	0.18	0.14	−0.30	0.32	0.08	0.09	−0.07	−0.23	0.27	0.33
SC	−0.03	0.21	1.00	−0.26	0.37	0.15	0.47	0.53	0.10	0.50	0.07	0.31	0.29	0.35	0.26	0.22
pH	0.30	0.04	−0.26	1.00	−0.04	0.01	−0.43	−0.53	0.07	−0.24	−0.31	−0.68	0.05	−0.40	0.32	0.04
Na	−0.25	0.36	0.37	−0.04	1.00	−0.64	0.46	0.13	−0.30	0.65	0.05	0.18	−0.38	−0.39	0.42	0.55
K	0.35	−0.24	0.15	0.01	−0.64	1.00	−0.12	0.05	0.49	−0.35	0.04	−0.09	0.45	0.46	−0.39	−0.57
Ca	−0.58	0.18	0.47	−0.43	0.46	−0.12	1.00	0.74	−0.36	0.56	0.21	0.52	−0.21	0.28	0.40	0.38
Mg	−0.57	0.14	0.53	−0.53	0.13	0.05	0.74	1.00	−0.39	0.49	0.12	0.60	0.04	0.50	0.36	0.29
Cl	0.56	−0.30	0.10	0.07	−.30	0.49	−0.36	−0.39	1.00	−0.37	0.07	−0.14	0.32	0.18	−0.39	−0.34
HCO_3	−0.35	0.32	0.50	−0.24	0.65	−0.35	0.56	0.49	−0.37	1.00	0.18	0.45	−0.11	−0.02	0.64	0.62
SO_4	−0.16	0.08	0.07	−0.31	0.05	0.04	0.21	0.12	0.07	0.18	1.00	0.43	0.14	0.04	0.08	0.16
NO3	−0.46	0.09	0.31	−0.68	0.18	−0.09	0.52	0.60	−0.14	0.45	0.43	1.00	−0.01	0.23	0.18	0.22
Fe	0.29	−0.07	0.29	0.05	−0.38	0.45	−0.21	0.04	0.32	−0.11	0.14	−0.01	1.00	0.42	0.01	−0.28
Mn	−0.16	−0.23	0.35	−0.40	−0.39	0.46	0.28	0.50	0.18	−0.02	0.04	0.23	0.42	1.00	0.08	−0.14
As	**−0.51**	**0.27**	**0.26**	**0.32**	**0.42**	**−0.39**	**0.40**	**0.36**	**−0.39**	**0.64**	**0.08**	**0.18**	**0.01**	**0.08**	**1.00**	**0.66**
F	−0.39	0.33	0.22	0.04	0.55	−0.57	0.38	0.29	−0.34	0.62	0.16	0.22	−0.28	−0.14	0.66	1.00
PD group																
E_H	1.00	0.94	−0.09	−0.10	−0.31	−0.89	0.14	−0.49	−0.09	−0.09	0.49	0.60	−0.37	−0.31	−0.37	−0.60
DO	0.94	1.00	−0.37	−0.35	−0.43	−0.77	−0.03	−0.71	−0.31	−0.37	0.60	0.49	−0.43	−0.43	−0.60	−0.66
SC	−0.09	−0.37	1.00	1.0	0.66	0.09	0.77	0.89	0.71	1.0	−0.26	0.31	0.26	0.66	0.58	0.37
pH	−0.10	−0.35	1.0	1.0	0.69	0.09	0.74	.89	0.73	1.0	−0.22	0.31	0.28	0.66	0.60	0.37
Na	−0.31	−0.43	0.66	0.69	1.00	0.54	0.83	0.54	0.49	0.66	−0.49	−0.26	0.71	1.0	0.49	0.71
K	−0.89	−0.77	0.09	0.09	0.54	1.00	0.14	0.37	0.09	0.09	−0.37	−0.60	0.49	0.54	0.14	0.60
Ca	0.14	−0.03	0.77	0.74	0.83	0.14	1.00	0.49	0.66	0.77	−0.20	0.14	0.49	0.83	0.20	0.26
Mg	−0.49	−0.71	0.89	0.88	0.54	0.37	0.49	1.00	0.60	0.88	−0.31	0.14	0.20	0.54	0.66	0.49
Cl	−0.09	−0.31	0.71	0.73	0.49	0.09	0.66	0.60	1.00	0.71	−0.60	−0.14	0.60	0.49	0.26	−0.03
HCO_3	−0.09	−0.37	1.0	1.0	0.66	0.09	0.77	0.89	0.71	1.00	−0.26	0.31	0.26	0.66	0.60	0.37
SO_4	0.49	0.60	−0.26	−0.22	−0.49	−0.37	−0.20	−0.31	−0.60	−0.26	1.00	0.77	−0.89	−0.49	−0.54	−0.43
NO_3	0.60	0.49	0.31	0.31	−0.26	−0.60	0.14	0.14	−0.14	0.31	0.77	1.00	−0.77	−0.26	−0.09	−0.31
Fe	−0.37	−0.43	0.26	0.28	0.71	0.49	0.49	0.20	0.60	0.26	−0.89	−0.77	1.00	0.71	0.31	0.43
Mn	−0.31	−0.43	0.66	0.66	1.0	0.54	0.83	0.54	0.49	0.66	−0.49	−0.26	0.71	1.00	0.49	0.71
As	**−0.37**	**−0.60**	**0.58**	**0.60**	**0.49**	**0.14**	**0.20**	**0.66**	**0.26**	**0.60**	**−0.54**	**−0.09**	**0.31**	**0.49**	**1.00**	**0.77**
F	−0.60	−0.66	0.37	0.37	0.71	0.60	0.26	0.49	−0.03	0.37	−0.43	−0.31	0.43	0.71	0.77	1.00

Table 4
Summary of major observation from the study area.

Parameters	RCD	YA	OA	PD
Aquifer composition	Channel sediments of Brahmaputra river	Younger alluvial recent flood plain of Brahmaputra	Older flood plain of Brahmaputra and its tributaries	Older flood plain of Brahmaputra and its tributaries
Major ion composition	Ca–HCO_3, Ca–Na–HCO_3, Na–Ca–HCO_3	Ca–Na–HCO_3	Na–Ca–HCO_3	Na–Ca–HCO_3
Major ion source	Carbonate rock (limestone and dolomite) and silicate rocks	Carbonate rock (limestone and dolomite) and silicate rocks (Ca-feldspar)	Siliceous sedimentary rocks (sandstone, shale), Himalayan argillaceous metamorphic rock	Siliceous sedimentary rocks (sandstone, shale), Himalayan argillaceous metamorphic rock
Weathering process	Carbonate dissolution and silicate weathering	Carbonate dissolution and silicate weathering	Silicate weathering	Silicate weathering
Groundwater As enrichment	Moderate Range (bdl–0.06 mg/L), Median (0.01 mg/L)	Low Range (bdl–0.05 mg/L), Median (>0.001 mg/L)	High Range (bdl–0.13 mg/L), Median (0.07 mg/L)	Lowest Range (bdl–0.04 mg/L), Median (0.01 mg/L)
Probable As mobilization mechanism	Reductive dissolution of Mn (oxy)hydroxide	Fe/Mn oxide/hydroxide reductive dissolution	pH dependent sorption, ionic competition	Ionic competition, pH

redox-sensitive parameters (e.g. Fe, Mn, SO_4^{2-}, NO_3) may be limited by the occurrence of multiple reactions in heterogeneous sediments (e.g. van Geen et al., 2004; Mukherjee and Fryar, 2008). On the backdrop of these observations, all of the groundwater samples show negative to very weak positive correlation of As with E_H ($\rho = 0.24$ to -0.51), which suggest that a redox-dependent mobilization play important role in As liberation. Arsenic shows negative correlation with pH in RCD and YA terrain however shows good correlation with pH ($\rho = 0.32$ and 0.60, respectively) in OA and PD terrains, suggesting that pH-dependent reactions are also potentially influencing factor in As mobilization in OA and PD terrains. Correlation between As and competitive anions HCO_3^- are negative in RCD and YA whereas strong positive correlation exist in OA and PD ($\rho = 0.64$ and 0.60, respectively) (Table 3). In the study area, Fe is positively correlated with As, in RCD ($\rho = 0.37$), YA ($\rho = 0.54$) and PD ($\rho = 0.31$) aquifers, but does not show any correlation in aquifers of OA terrain ($\rho = 0.014$) (Table 3). Likewise, Mn showed strong positive correlation for RCD ($\rho = 0.72$) and moderately positive for YA ($\rho = 0.54$) and PD ($\rho = 0.49$). The groundwater of all terrains show very weak positive to negative correlation between As and SO_4^{2-} ($\rho = 0.08$ to -0.54) (Table 3), which reaffirms that pyrite/sulfide oxidation is not the governing process for As liberation/mobilization. Accordingly, the calculation of nonparametric correlation suggested that multiple hydrogeochemical processes controls As fate in the present study area, and no single process can be identified to be predominating the system (Table 4).

4.5.3. Arsenic fate: Possible mobilization mechanism and distribution

Because of proximity, similar aquifer sediment source (i.e. the Himalayas), climatic condition and land use, groundwater As enrichment in the study area can be explained on the basis of already proposed hypotheses for Bengal basin and Central Gangetic plain (e.g. Bhattacharya et al., 1997; Ravenscroft et al., 2001; Harvey et al., 2002; Chatterjee et al., 2003; Zheng et al., 2004; Gault et al., 2005; Mukherjee et al., 2011, 2012). Some authors have proposed that As could be mobilized from the oxidation of As-enriched pyrite (Das et al., 1996) and other proposed the importance of reductive dissolution of metal (Fe/Mn) oxide/hydroxide and subsequent release of the adsorbed As, in the process of its mobilization (Bhattacharya et al., 1997; Zheng et al., 2004). Possible mechanisms controlling arsenic distribution in the study area can be envisioned in light of the sediment provenance

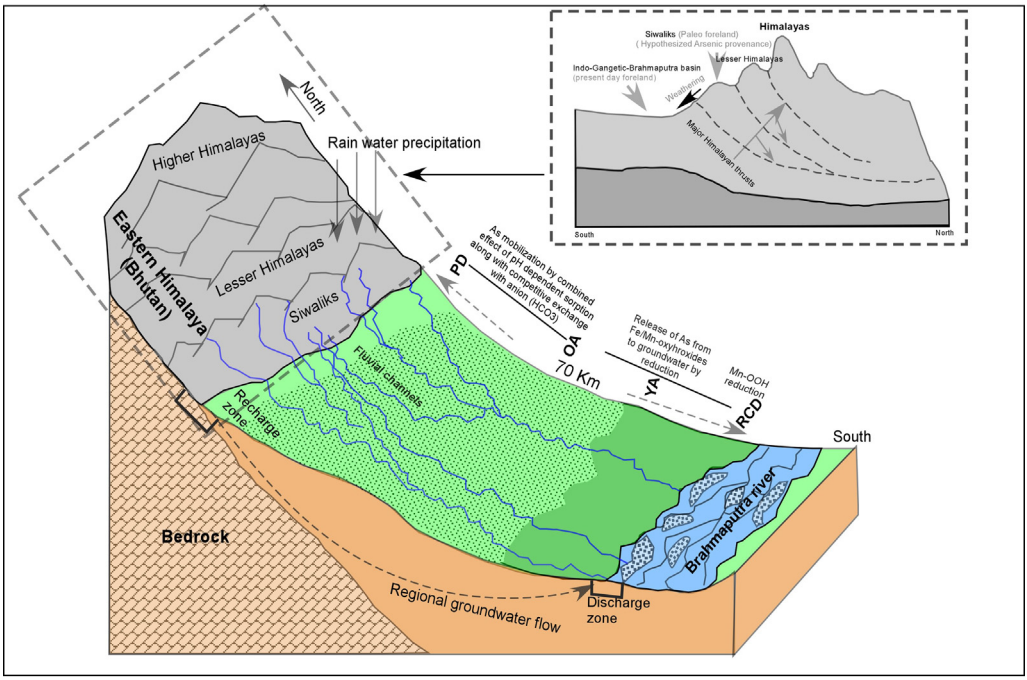

Fig. 12. Plots showing As mobilization mechanism in groundwater of four different alluvial terrains (RCD, YA, OA and PD).

and geochemistry of the four studied terrains. As discussed in the previous sections, very high concentrations of Fe and low concentrations of SO_4^{2-} are observed in the groundwater of all studied terrains. In RCD terrain, As shows more prominent correlation with Mn ($\rho = 0.72$) and less with Fe ($\rho = 0.37$), suggesting Mn–OOH reduction and dissolution leading to liberation of Mn and As could be a more dominant process (Fig. 12). Similarly, in YA terrain, groundwater As showed good positive correlation with Fe and Mn which suggests that reduction of Fe/Mn oxyhydroxides is the possible mechanism of As liberation in the aquifers. In OA and PD terrains, groundwater As shows positive correlation with pH and HCO_3^-, suggests that As could be mobilized by combined effect of pH and bicarbonate and pH dependent sorption play an important role in As liberation.

Thus, the above noted mechanisms can lead to high As liberation in aquifers of four different geomorphic terrains (Fig. 12). Hence, it might be summarized that As liberation in the aquifers of the study area are related to redox transitions between solid-phase As-bearing minerals in aquifer sediments and circulating groundwater in a dominantly reducing condition.

5. Conclusion

Hydrogeochemistry, chemical evolution and As distribution are investigated in aquifers of four different geomorphologic terrains, which extend from northern bank of Brahmaputra river to the foothills of Eastern Himalayas. Previous studies in the adjoining Central Gangetic plains and Bengal basin have demonstrated distinct influence of geology and geomorphology on solute composition and groundwater As distribution in the aquifers. The present study investigates such influence in the aquifers of the Brahmaputra basin, whose evolution is more intricately related to the tectonomorphic evolution of the Himalayas, than the downstream Gangetic basin aquifers. The study area has been classified into four geomorphic units viz. river channel deposits (RCD), younger alluvium (YA), older alluvium (OA) deposits and piedmont deposits (PD). Plots of major ions suggested that groundwater is dominated by Ca–Na–HCO_3 and Na–Ca–HCO_3 hydrogeochemical facies. Major ion chemistry data showed

that Ca^{2+} dominated groundwater in RCD and YA terrain and are probably derived from carbonate dissolution and Ca-silicate weathering. Analyses show groundwater samples of OA and PD terrains are within or close to the global-average silicate weathering domain, suggesting leaching of lithotypes derived from argillaceous metamorphic rock and weathering of feldspar minerals dominantly present in Lesser Himalayas and carried by northern tributaries of the Brahmaputra river. Molar ratio calculations suggest that cation exchange has no influence on the groundwater chemistry of the study area, possibly since the aquifers are closer to the recharge domains, i.e. shorter flow path and lower groundwater residence time. On the basis of this observation, mineral weathering is identified as the dominant mechanism in evolution and source of cations in the groundwater of study area. According to stable isotope composition, groundwater of these groups indicates that some evaporation may have taken place through recharging water in study area. Field parameters and laboratory analyses showed that all groundwater samples fall in the postoxic subgroup of anoxic environment. Dissolve As concentrations ranged from <0.001 to 0.13 mg/L (mean 0.023 mg/L) in the groundwater of different alluvial terrains where OA terrain shows the highest concentration. The aquifers of YA and RCD terrains are moderately As enriched and samples of PD terrain are least contaminated. Spearman's rho (ρ) calculation of bivariate relationship between As and other hydrogeochemical parameters indicates As is showing positive correlation with redox-sensitive parameter like (Fe and Mn) in RCD and YA terrains thus suggest reductive dissolution of (Fe–Mn)OOH could be the dominant mechanism. In OA and PD terrains, As showed positive correlation with competitive anions (HCO_3^-) and pH. This suggests that As may be mobilized by combined effect of pH dependent sorption along with competitive exchange with anion (HCO_3^-). Therefore, As distribution and mobilization processes in the recharge areas, which are situated near or very close to the Himalayan foothills, differ from those in the discharge areas, i.e. located near the main channel of Brahmaputra river and alluvial deposits.

Acknowledgements

SV acknowledges CSIR (Government of India) for providing CSIR-SR Fellowship. The authors acknowledges support of IIT Guwahati for carrying out fieldwork and IIT Kharagpur for providing laboratory analyses facilities. The authors are thankful to Palash Debnath and Soumendra Nath Bhanja, IIT Kharagpur for their technical support and help in samples analyses part.

References

Acharyya, S.K., Shah, B.A., 2007. Groundwater arsenic contamination affecting different geologic domains in India—a review: influence of geological setting, fluvial geomorphology and Quaternary stratigraphy. J. Environ. Sci. Health A 42, 1795–1805.

Anawar, H.M., Akai, J., Komaki, K., Terao, H., Yoshioka, T., Ishizuka, T., Safiullah, S., Kato, K., 2003. Geochemical occurrence of arsenic in groundwater of Bangladesh: sources and mobilization processes. J. Geochem. Explor. 77, 109–131.

Ahmed, K.M., Bhattacharya, P., Hasan, M.A., Akhter, S.H., Alam, S.M., Bhuyian, M.A.H., Imam, M.B., Khan, A.A., Sracek, O., 2004. Arsenic enrichment in groundwater of the alluvial aquifers in Bangladesh: an overview. Appl. Geochem. 19, 181–200.

Bhattacharya, P., Chatterjee, D., Jacks, G., 1997. Occurrence of arsenic-contaminated groundwater in alluvial aquifers from the Bengal Delta Plain, Eastern India: options for a safe drinking water supply. Water Resour. Dev. 13, 79–92.

Bhattacharya, P., Jacks, G., Ahmed, K.M., Routh, J., Khan, A.A., 2002. Arsenic in Groundwater of the Bengal Delta Plain Aquifers in Bangladesh. Bull. Environ. Contam. Toxicol. 69, 538–545.

Bhattacharya, P., Jacks, G., Jana, J., Sracek, A., Gustafsson, J.P., Chatterjee, D., 2001. Geochemistry of the Holocene alluvial sediments of Bengal Delta Plain from West Bengal, India: implications on arsenic contamination in groundwater. Groundwater arsenic contamination in the Bengal Delta Plain of Bangladesh 3084, 21–40.

Bhattacharya, P., Claesson, M., Bundschuh, J., Sracek, O., Fagerberg, J., Jacks, G., Thir, J.M., 2006. Distribution and mobility of arsenic in the Rio Dulce alluvial aquifers in Santiago del Estero Province, Argentina. Sci. Total Environ. 358 (1), 97–120.

Bhattacharya, P., Mukherjee, A., Mukherjee, A.B., 2011. Arsenic contaminated groundwater of India. In: Nriagu, J. (Ed.), Encyclopedia of Environmental Health. Elsevier B.V., Netherlands, pp. 150–164.

Biswas, A., Majumder, S., Neidhardt, H., Halder, D., Bhowmick, S., Mukherjee-Goswami, A., Kundu, A., Saha, D., Berner, Z., Chatterjee, D., 2011. Groundwater chemistry and redox processes: depth dependent arsenic release mechanism. Appl. Geochem. 26, 516–525.

Böttcher, J., Strebel, O., Voerkelius, S., Schmidt, H.L., 1990. Using isotope fractionation of nitrate–nitrogen and nitrate–oxygen for evaluation of microbial denitrification in sandy aquifer. J. Hydrol. 114, 413–424.

Charlet, L., Polya, D.A., 2006. Arsenic in shallow, reducing groundwater in southern Asia: an environmental health disaster. Elements 2, 91–96.

Chatterjee, D., Chakraborty, S., Nath, B., Jana, J., Bhattacharyya, R., Mallik, S.B., Charlet, L., 2003. Mobilization of arsenic in sedimentary aquifer vis-a-vis subsurface iron reduction processes. J. Phys. IV Proc. 107, 293–296 (EDP sciences).

Chatterjee, D., Halder, D., Majumder, S., Biswas, A., Nath, B., Bhattacharya, P., Bundschuh, J., 2010. Assessment of arsenic exposure from groundwater and rice in Bengal Delta Region, West Bengal, India. Water Res. 44 (19), 5803–5812.
Chetia, M., Chatterjee, S., Banerjee, S., Nath, J., Singh, L., Srivastava, B., Sarma, P., 2011. Groundwater arsenic contamination in Brahmaputra river basin: a water quality assessment in Golaghat (Assam), India. Environ. Monit. Assess. 173, 371–385.
Coleman, J.M., 1969. Brahmaputra River: channel processes and sedimentation. Sediment. Geol. 3 (2), 129–239.
Craig, H., 1961. Isotopic variations in meteoric water. Science 133, 1702–1703.
Das, D., Samanta, G., Mandal, B.K., Chowdhury, T.R., Chanda, C.R., Chowdhury, P.P., Chakraborti, D., 1996. Arsenic in groundwater in six districts of West Bengal, India. Environ. Geochem. Health 18 (1), 5–15.
Diwakar, J., Johnston, S.G., Burton, E.D., Shrestha, S., 2015. Arsenic mobilization in an alluvial aquifer of the Terai region, Nepal. J. Hydrol.: Reg. Stud. 4, 59–79.
Dowling, C.B., Poreda, R.J., Basu, A.R., Peters, S.L., Aggarwal, P.K., 2002. Geochemical study of arsenic release mechanisms in the Bengal Basin groundwater. Water Resour. Res. 38 (9), 1–18.
Drever, J.I., 1997. The Geochemistry of Natural Waters, 3rd ed. Prentice-Hall, Upper Saddle River, NJ, pp. 388.
Enmark, G., Nordborg, D., 2007. Arsenic in the groundwater of the Brahmaputra floodplains, Assam, India – Source, distribution and release mechanisms. In: Minor Field Study 131. Uppsala University, Sweden, ISSN 1653-5634.
Gaillardet, J., Dupre, B., Louvat, P., Allegre, C.J., 1999. Global silicate weathering and CO_2 consumption rates deduced from the chemistry of large rivers. Chem. Geol. 159, 3–30.
Garrels, R.J., MacKenzie, F.T., 1971. Evolution of Sedimentary Rocks. Norton, New York.
Garzanti, E., Vezzoli, G., Andó, S., France-Lanord, C., Singh, S.K., Foster, G., 2004. Sand petrology and focused erosion in collision orogens: the Brahmaputra case. Earth Planet. Sci. Lett. 220, 157–174.
Gault, A.G., Islam, F.S., Polya, D.A., Charnock, J.M., Boothman, C., Chatterjee, D., Lloyd, J.R., 2005. Microcosm depth profiles of arsenic release in a shallow aquifer, West Bengal. Mineral. Mag. 69 (5), 855–863.
Guillot, S., Charlet, L., 2007. Bengal arsenic, an archive of Himalaya orogeny and paleohydrology. J. Environ. Sci. Health A 42, 1785–1794.
Harvey, C.F., Swartz, C.H., Badruzzaman, A.B.M., Keon-Blute, N., Yu, W., Ali, M.A., Jay, J., Beckie, R., Niedan, V., Brabander, D., Oates, P.M., Ashfaque, K.N., Islam, S., Hemond, H.F., Ahmed, M.F., 2002. Arsenic mobility and groundwater extraction in Bangladesh. Science 298, 1602–1606.
Heroy, D.C., Kuehl, S.A., Goodbred, S.L., 2003. Mineralogy of the Ganges and Brahmaputra Rivers: implications for river switching and Late Quaternary climate change. Sed. Geol. 155, 343–359.
Islam, F.S., Gault, A.G., Boothman, C., Polya, D.A., Charnock, J.M., Chatterjee, D., Lloyd, J.R., 2004. Role of metal-reducing bacteria in arsenic release from Bengal delta sediments. Nature 430 (6995), 68–71.
Langmuir, D., 1971. The geochemistry of some carbonate ground waters in central Pennsylvania. Geochim. Cosmochim. Acta 35 (10), 1023–1045.
Lang, K.A., Huntington, K.W., 2014. Antecedence of the Yarlung–Siang–Brahmaputra River, eastern Himalaya. Earth Planet. Sci. Lett. 397, 145–158.
Mahanta, C., Enmark, G., Nordborg, D., Sracek, O., Nath, B.N., Nickson, R.T., Herbert, R., Jacks, G., Ramanathan, A.L., Mukherjee, A., Bhattacharya, P., 2015. Understanding distribution, hydrogeochemistry and mobilization mechanism of arsenic in groundwater in a low-industrialized homogeneous part of Brahamputra river floodplain. India, Journal of Hydrology: Regional Studies, this issue.
Meybeck, M., 1987. Global chemical weathering from surficial rocks estimated from river dissolved loads. Am. J. Sci. 287, 401–428.
Mukherjee, A., Fryar, A.E., 2008. Deeper groundwater chemistry and geochemical modeling of the arsenic affected western Bengal basin, West Bengal, India. Appl. Geochem. 23, 863–892.
Mukherjee, A., Bhattacharya, P., Savage, K., Foster, A., Bundschuh, J., 2008. Distribution of geogenic arsenic in hydrologic systems: controls and challenges. J. Contam. Hydrol. 99, 1–7.
Mukherjee, A., Stewart, S., Lyster, S., Riddel, J., Rostron, B., 2010. Effect of sub-hydrostatic conditions on basin-scale groundwater flow in the southern portion of the Canadian Rockies Foreland Basin. Geol. Soc. Am. Abs. 42 (5), 432.
Mukherjee, A., Fryar, A.E., Scanlon, B.R., Bhattacharya, P., Bhattacharya, A., 2011. Elevated arsenic in deeper groundwater of western Bengal basin, India: extents and controls from regional to local-scale. Appl. Geochem. 26, 600–613.
Mukherjee, A., Saha, D., Harvey, C.F., Taylor, R.G., Ahmed, K.M., Bhanja, S.N., 2015. Groundwater systems of the Indian Sub-Continent. J. Hydrol.: Reg. Stud. 4, 1–14.
Mukherjee, A., Scanlon, B., Fryar, A., Saha, D., Ghoshe, A., Chowdhuri, S., Mishra, R., 2012. Solute chemistry and arsenic fate in aquifers between the Himalayan foothills and Indian craton (including central Gangetic plain): influence of geology and geomorphology. Geochim. Cosmochim. Acta 90, 283–302.
Mukherjee, A., Verma, S., Gupta, S., Henke, K.R., Bhattacharya, P., 2014. Influence of tectonics, sedimentation and aqueous flow cycles on the origin of global groundwater arsenic: paradigms from three continents. J. Hydrol. 518, 284–299.
Naidu, R., Bhattacharya, P., 2009. Arsenic in the environment—risks and management strategies. Environ. Geochem. Health 31, 1–8.
Nath, B., Berner, Z., Mallik, S.B., Chatterjee, D., Charlet, L., Stueben, D., 2005. Characterization of aquifers conducting groundwaters with low and high arsenic concentrations: a comparative case study from West Bengal, India. Mineral. Mag. 69 (5), 841–854.
Nriagu, J.O., Bhattacharya, P., Mukherjee, A.B., Bundschuh, J., Zevenhoven, R., Loeppert, R.H., 2007. Arsenic in soil and groundwater: an overview. Trace Metals and other Contaminants in the Environment 9, 3–60.
Parkhurst, D.L., Christenson, S., Breit, G.N., 1996. Ground-water quality assessment of the Central Oklahoma aquifer, Oklahoma-geochemical and geohydrologic investigations. U.S. Geological Survey Water-Supply Paper 2357-C, 101 pp.
Postma, D., Jakobsen, R., 1996. Redox zonation: equilibrium constraints on the Fe(III)/SO4-reduction interface. Geochim. Cosmochim. Acta 60 (17), 3169–3175.
Rahman, M.M., Naidu, R., Bhattacharya, P., 2009. Arsenic contamination in groundwater in the Southeast Asia region. Environ. Geochem. Health 31, 9–21.

Ravenscroft, P., McArthur, J.M., Hoque, B., 2001. Geochemical and palaeohydrological controls on pollution of groundwater by arsenic. In: Chappell, W.R., Abernathy, C.O., Calderon, R. (Eds.), Arsenic Exposure and Health Effects IV. Elsevier Science Ltd., Oxford, pp. 53–77.
Ravenscroft, P., Brammer, H., Richards, K.S., 2009. Arsenic Pollution: A Global Synthesis. Wiley-Blackwell, Chichester, UK.
Saunders, J.A., Lee, M.-K., Uddin, A., Mohammad, S., Wilkin, R.T., Fayek, M., Korte, N.E., 2005. Natural arsenic contamination of Holocene alluvial aquifers by linked tectonic, weathering, and microbial processes. Geochem. Geophys. Geosyst. 6, Q04006, http://dx.doi.org/10.1029/2004GC000803.
Singh, S., 2005. Spatial variability in erosion in the Brahmaputra basin: causes and impacts. Curr. Sci. 90 (9), 1272–1275.
Smedley, P.L., Kinniburgh, D.G., 2002. A review of the source, behavior and distribution of arsenic in natural waters. Appl. Geochem. 17, 517–568.
Smedley, P.L., 2005. Arsenic occurrence in groundwater in South and East Asia-scale, causes and mitigation. In: Towards a More Effective Operational Response: Arsenic Contamination of Groundwater in South and East Asian Countries, Volume II Technical Report, World Bank Report No. 31303.
Stanger, G., 2005. A palaeo-hydrogeological model for arsenic contamination in southern and south-east Asia. Environ. Geochem. Health 27 (4), 359–368.
Stüben, D., Berner, Z., Chandrasekharam, D., Karmakar, J., 2003. Arsenic enrichment in groundwater of West Bengal, India: geochemical evidence for mobilization of As under reducing conditions. Appl. Geochem. 18 (9), 1417–1434.
Ward, J.H., 1963. Hierarchical grouping to optimize an objective function. J. Am. Stat. Assoc. 69, 236–244.
Wood, W.W., 1981. Guidelines for collection and field analysis of ground-water samples for selected unstable constituents. In: US Geol. Surv. Techniques Water-Resour. Invest. Book 1 (Chapter D2).
van Geen, A., Rose, J., Thoral, S., Garnier, J.M., Zheng, Y., Bottero, J.Y., 2004. Decoupling of As and Fe release to Bangladesh groundwater under reducing conditions. Part II. Evidence from sediment incubations. Geochim. Cosmochim. Acta 68, 3475–3486.
Zheng, Y., Stute, M., Van Geen, A., Gavrieli, I., Dhar, R., Simpson, H.J., Ahmed, K.M., 2004. Redox control of arsenic mobilization in Bangladesh groundwater. Appl. Geochem. 19 (2), 201–214.